THEORETICA CHIMICA ACTA

Theoret. Chim. Acta (Berl.) 59, 569–583 (1981)

The Band Structure and Magnetic Properties of Some Transition-metal Phosphides. II. V, Cr, and Mn Monophosphides

Peter G. Perkins, Ashok K. Marwaha, and James J. P. Stewart

Department of Pure and Applied Chemistry, University of Strathclyde, Glasgow G1 1XL, Scotland

The band structures and density of states for VP, CrP, and MnP are calculated by an LCAO-TB method. The results allow interpretation of the metallic nature of the materials, the trend in magnetic properties observed, and the bonding in such binary phosphides.

Key words: Band structure – Binary phosphides – Magnetic properties.

1. Introduction

A previous paper [1] has dealt with the electronic band structure of scandium phosphide and has discussed the origin of the observed properties of this material.

Other transition-metal monophosphides also possess interesting electrical and magnetic properties, e.g., only MnP has been shown to be magnetic below 292 K [2], the other members of the series possessing merely weak Pauli paramagnetism.

Stein and Walmsley [2] have offered a qualitative explanation for the magnetic behaviour of these compounds: this is based on the approach of Goodenough [3].

Goodenough's theory for the transition-metal monophosphides is based on his interpretation of transition-metal oxides. The basic assumption is that a formal valence state of $M^{3+}P^{3+}$ is approximately correct and so the $3d$ metal states lie in a gap between the occupied phosphorus $3s$ and $3p$ valence bands and an empty conduction band. The non-cubic component of the crystal field splits up the e_g states (which are directed towards the anions) and the t_{2g} states. The latter are involved in the metal-metal bonding. Those states on atoms for which the intermetallic distance R is less than a critical value R_c are considered banded

0040-5744/81/0059/0569/$03.00

and their electrons itinerant. The value of R_c is determined semi-empirically. These considerations lead to schematic band structures. For vanadium phosphide, with NiAs structure, all the metal-metal distances are less than the semi-empirical value of R_c: this results in banded states. The position of the Fermi level is then supposed to give rise to small Pauli paramagnetism.

The remaining phosphides have the B31 MnP structure. In this case, the inherent orthombic distortion splits any remaining degeneracies. Because of the distortion, the metal-metal distances are altered such that both $R < R_c$ and $R > R_c$ may be found. Hence, both overlapping bands and localised states are formed. The partial occupation of these localised states induces an intra-atomic exchange splitting and, depending on the magnitude of this splitting, the compound may be in either a high-or a low-spin state. The saturation moment of MnP (1.29 μB) [2] indicates it a low-spin state.

Because the above considerations depend critically on an assumed knowledge of the nature of the bonding, then we would expect that band-structure calculations should give a more soundly based rationale of the magnetic properties than does a semi-intuitive explanation. To this end, therefore, we chose three members of the series, namely, VP, CrP, and MnP for the band-structure calculations.

2. Method of Calculation

2.1. Crystal Structures

VP has NiAs structure (Fig. 1), where the phosphorus octahedron shares faces which are perpendicular to the c axis. There are two molecules per unit cell. CrP, MnP, FeP, and CoP all have $B31$ MnP structure with four molecules per unit cell. This structure is derived from an orthorhombic distortion of the NiAs lattice by displacement of the phosphorus atoms by a small amount along the c-axis and of the metal atoms normal to the c-axis, resulting in their movement out of the centres of the phosphorus octahedra. The structure is shown in Fig. 2. The lattice parameters [4, 5, 6] and space group for the solids studied are given in Table 1.

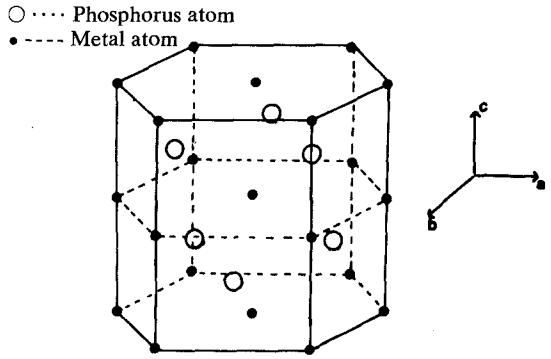

Fig. 1. Crystal structure of VP

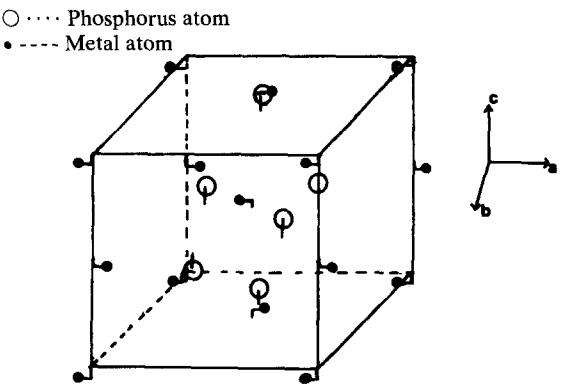

Fig. 2. The $B31$ MnP structure

Table 1. Lattice parameters and space groups for VP, CrP, and MnP (Å)

	a	b	c	Group
VP	3.178	3.178	6.244	D_{6h}^4
CrP	5.362	3.113	6.018	D_{2h}^{16}
MnP	5.258	3.172	5.918	D_{2h}^{16}

2.2. Band Structure and Density-of-States

The method used for band-structure calculations was based on the Extended-Hückel formulation previously discussed [1]. Input atomic data (orbital exponents and valence-state ionisation potentials for the basis functions) are in Table 2 for all the elements.

For the $B31$ structures the number of valence orbitals per unit cell amounts to 72 if the empty phosphorus $3d$ orbitals are included. This size of basis set is unmanageable and, hence, we were compelled to neglect the phosphorus $3d$ orbitals in all cases. In every instance the Mulliken–Wolfsberg–Helmholtz scaling

Table 2. Input atomic data

	Orbital exponents[a]				V.S.I.P.[b]		
	$4s$		$4p$	$3d$	$4s$	$4p$	$3d$
V	1.20		0.80	2.50	6.32	3.47	6.32
Cr	1.30		0.83	2.65	6.57	3.47	7.93
Mn	1.45		0.95	2.93	6.82	3.60	7.93
P	(3s) 1.75		(3p) 1.30	—	19.37	10.84	—

[a] Calculated from Burns Rules [13].
[b] Calculated from atomic spectra in the usual way.

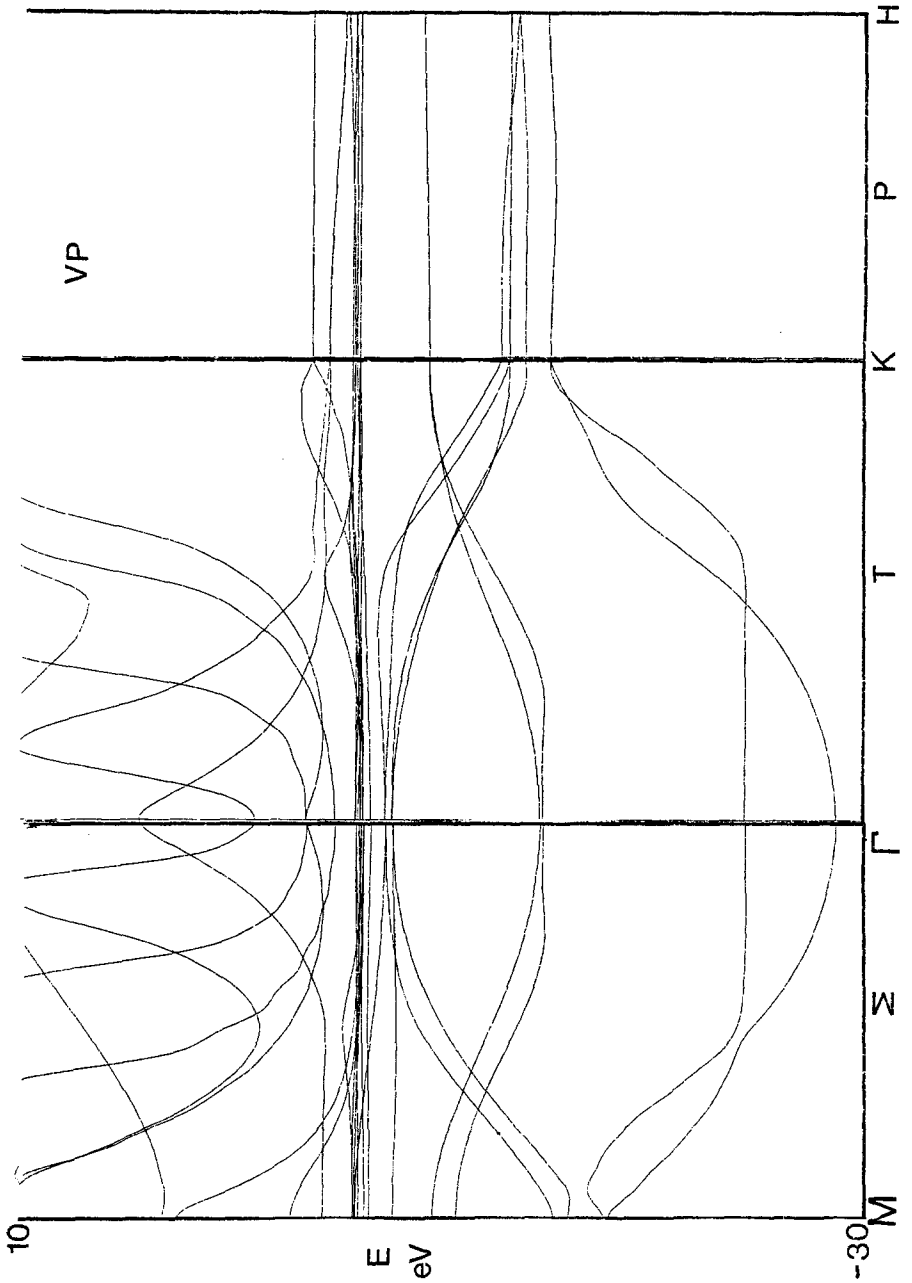

Fig. 3. General band structure for VP between points $M\Gamma KH$

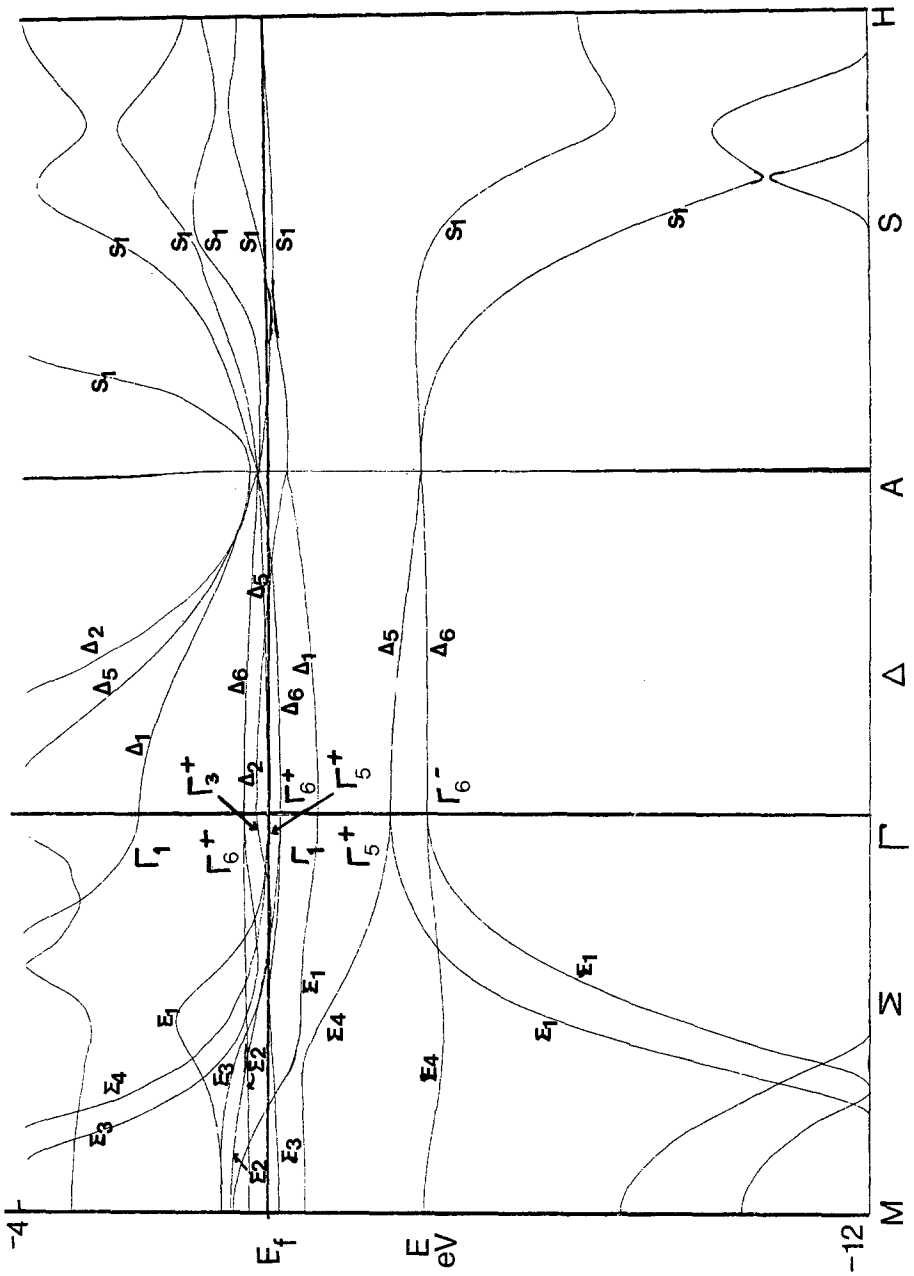

Fig. 4. Expanded band structure for VP ($M\Gamma AH$)

factor for the off-diagonal matrix elements between atomic orbitals was set at 2.0. When such large basis sets are used, there ensues the problem of correctly connecting up the points in k-space given by the calculation and correctly identifying crossing points. This task was carried out automatically, as detailed previously [1]. The density-of-states and related functions were obtained using linear interpolation techniques as before [1].

3. Results and Discussion

3.1. Band Structure for VP

Interactions between 27 unit cells were taken into account for the calculation. The first Brillouin Zone for the hexagonal lattice is hexagonal and in our results we follow the notation of Herring [7] for the high-symmetry points.

Fig. 3 shows the band structure along the continuous lines M-Γ-K-H in the energy range −30.0 eV to 10.0 eV.

Fig. 4 shows an exemplary expanded band structure in the energy region −12.0 eV to −4.0 eV along the symmetry lines M-Γ-A-H. For brevity, the rest is not reproduced here. There is a marked difference between the band structures of ScP [1] and VP. Whereas, in the case of ScP, the valence and conduction bands are separated by an energy gap, in VP the bands overlap and the gap disappears. Table 3 shows the composition of the valence band at the point Γ of the Zone and illustrates mixing of the metal-ligand orbitals. The energy bands arising from the 3d orbitals of vanadium are clustered in a narrow energy range centred at −6.00 eV. The extra two electrons that VP possesses over ScP move the Fermi Level higher up in the energy scale. The Fermi level now lies in the region of the bands arising from the 3d orbitals of vanadium at −6.32 eV and crosses five bands. This results in several different large areas of Fermi surface and the material will clearly be a metallic conductor.

Figs. 5–7 show three of the Fermi surfaces constructed from the band-structure. There are both electron and hole surfaces, suggesting both positive and negative

Table 3. Composition of the valence band in VP at the point Γ

Energy (eV)	Symmetry	Composition
−28.71	Γ_4^-	93% 3s (P), 7% 4p (V)
−24.42	Γ_1^+	59% 3p (P), 40% 4s (V), 1% 3d (V)
−14.92	Γ_3^+	69% 3p (P), 31% 4s (V)
−14.77	Γ_2^-	97% 3p (P), 3% 4p (V)
−7.82	Γ_6^-	13.5% 3p (P), 86.5% 4p (V)
−7.48	Γ_5^+	13.5% 3p (P), 86.5% 4p (V)
−6.79	Γ_1^+	100% 3d (V)
−6.44	Γ_6^+	100% 3d (V)
−6.32	Γ_5^+	0.6% 3p (P), 99.4% 3d (V)

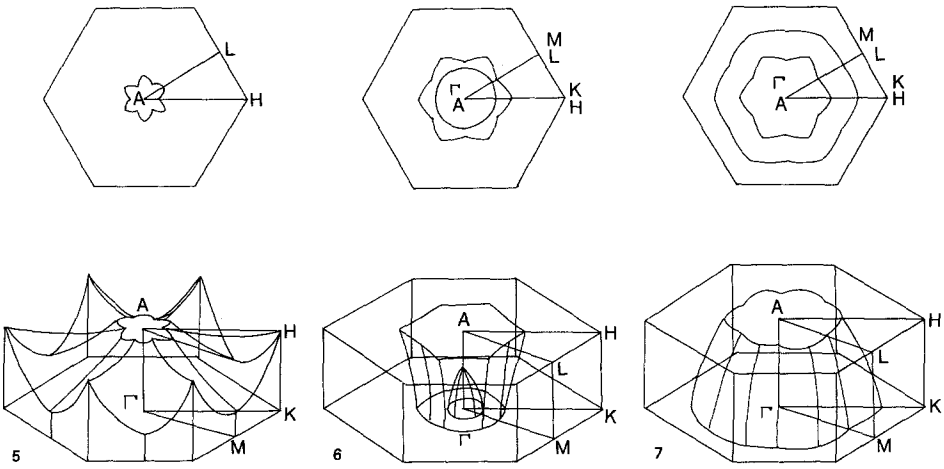

Figs. 5, 6, 7. Fermi surfaces for VP

effective-mass tensor components. The picture is, of course, only qualitative but the large open-orbit Fermi surfaces in both longitudinal and transverse directions suggest basically similar conductivities in the respective directions. Because of the necessary uncertainty in the shapes of the bands around the Fermi level, we have not considered it worthwhile to derive the effective electron masses for each open band. However, the general width and curvature of the bands for the three materials show that the effective masses will be in the order $V \ll Cr < Mn$.

3.2. Band Structures for CrP *and* MnP

The primitive unit cell of the MnP structure contains four molecules but, as in VP, interactions between 27 unit cells were taken into account and the input parameters for the basis set are given in Table 2. The central Brillouin Zone for this lattice is also orthorhombic and the notation of Koster [7] for high-symmetry points is appropriate.

Parts of the energy band structures for CrP and MnP are shown in Figs. 8 and 9. Both compounds show clustering of the bands arising from $3d$ orbitals of transition metal over a very narrow energy range centred at about -7.6 eV. The wavefunctions examined at various points in the Brillouin Zone suggest a considerable amount of mixing between the metal and ligand orbitals. They also show some s and p character in the wavefunctions forming bands near the Fermi level. The Fermi level in both these cases lies in the bands arising from the $3d$ orbitals of the metal at -7.79 eV and -7.86 eV for CrP and MnP, respectively. The large number of bands crossing the Fermi level in both these cases correlates with the metallic nature of these materials. Since the band structures for both these materials contain twice as many bands as does VP, then the Fermi surfaces are clearly more numerous and more complex. The necessary uncertainties in

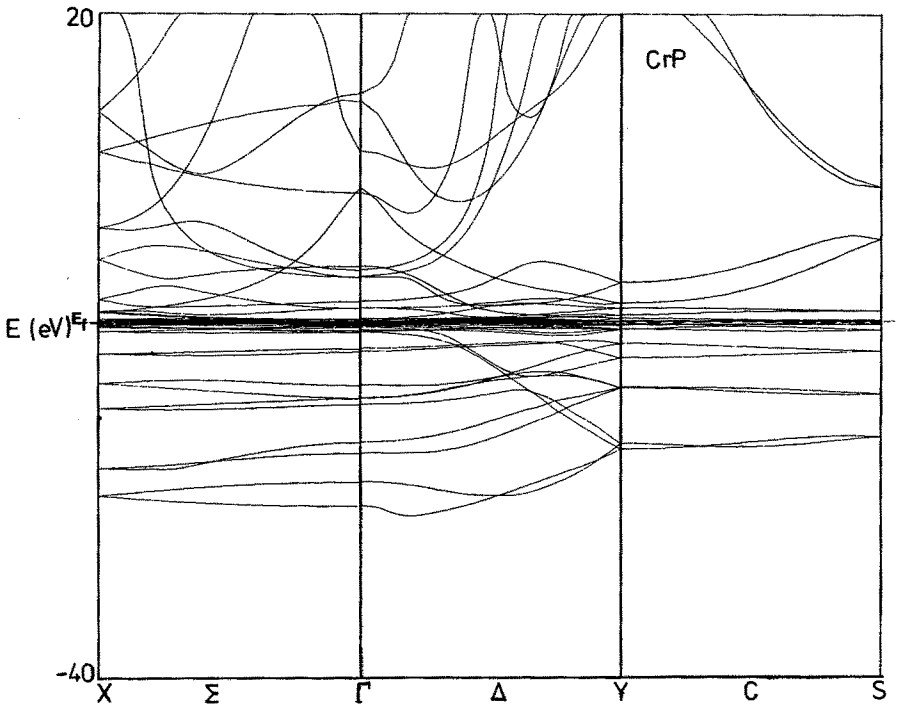

Fig. 8. General band structure for CrP between points *X*-Γ-*Y*-*S*

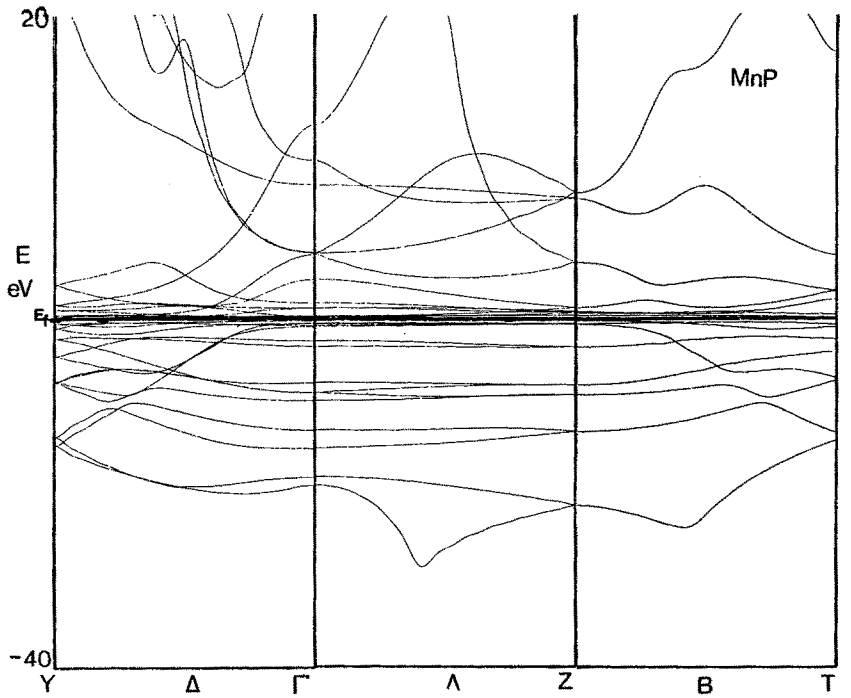

Fig. 9. General band structure for MnP between points (*XΓZT*)

the calculational procedure, however, render the detailed analysis of these surfaces unprofitable.

The chief point which emerges from the band structures is the nature of the bands at the Fermi surface, i.e., these surfaces lie within a densely grouped, narrow, mainly *d*-band region.

3.3. The Density-of-States and Related Functions for VP, CrP, *and* MnP

One can get further insight into the physical properties of these materials by examination of the density-of-states functions in the Fermi level region. These are given in Figs. 10–12.

Firstly, we present a semi-quantitative argument based on the total density of states for the paramagnetic behaviour of these materials. The spin susceptibility χ_p of a free electron gas is given by [8]

$$\chi_p = \mu_0^2 G(E_f)$$

where μ_0 and $G(E_f)$ are the magnetic moments of the electron and the density-of-states at the Fermi level, E_f, respectively. We can use this equation for the ee-electron gas to obtain approximate spin susceptibilities of these mono-phosphides. In general, of course, the exchange interactions involved in the real systems will modify the value of χ_p by favouring the parallel spins. Table 4 gives an estimate of χ_p from Figs. 10 to 12, and of $G(E_f)$ and ΔE_f (the half-band width

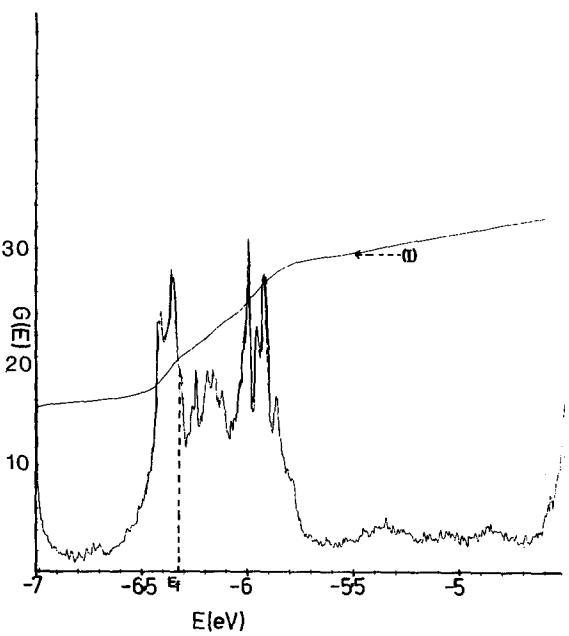

Fig. 10. Density-of-states for VP near E_f on an expanded scale. The curve marked (I) is the integral of $G(E)$ and the abscissa gives the number of electrons

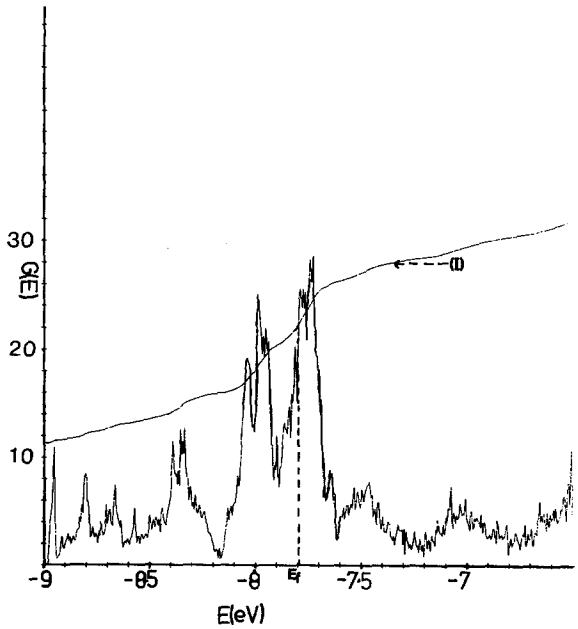

Fig. 11. Density-of-states for CrP near E_f on an expanded scale

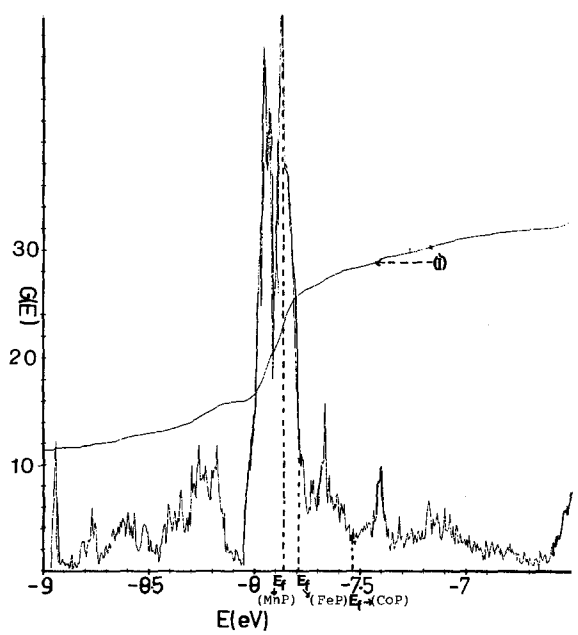

Fig. 12. Density-of-states for MnP on an expanded scale. Projected Fermi energies for FeP and CoP are also indicated

Table 4. ΔE_f, the half-band width near E_f and $G(E_f)$ for VP, CrP, and MnP calculated on a relative scale

MP	ΔE_f	$G(E_f)$
VP	0.55 eV	1.0
CrP	0.35 eV	1.25
MnP	0.20 eV	3.2

near E_f) on a relative scale. The former (GE_f) are taken from density-of-states curves and scaled to correspond to one molecule of MP per unit volume. We use Table 4 along with the density-of-states curves to consider the magnetic susceptibilities of these compounds.

Vanadium phosphide and chromium phosphide (Figs. 10 and 11) exhibit a low value of the density-of-states near E_f. Taken together, $G(E_f)$ and ΔE_f for VP and CrP shown in Table 4 suggest temperature-independent spin-only magnetic susceptibilities for these materials.

Fig. 12 shows the density-of-states function for MnP near the Fermi level, E_f. The large value of 3.2 for the relative $G(E_f)$ and the small value of 0.20 eV for ΔE_f suggest that the exchange energy will be high, thus favouring spin alignment and resulting in a magnetic material with susceptibility, χ_p, of the order of 100 times that found in VP and CrP.

The results obtained above are in agreement with the magnetic susceptibilities obtained experimentally by Stein and Walmsley for these compounds [2]. Furthermore, one can also make projections for the magnetic susceptibilities of FeP and CoP, making the reasonable assumption that the overall shape of $G(E)$ for the $B31$ MnP structure is similar for these two phosphides. Addition of one and two electrons, respectively, yields positions of E_f for FeP and CoP shown in Fig. 12. From this we predict that the value of spin-only χ_p for FeP will be similar to that of CrP whereas, in the case of CoP, χ_p will be very small and will result essentially from complete filling of the $3d$ bands. The above trend was also found in the magnetic susceptibilities of CoP and FeP by Stein and Walmsley [2].

Secondly, we can use the density-of-states functions to rationalise the order of the metallic conductivities, σ, found for these compounds. The extended-band specific electrical conductivity, σ, can be expressed as a function of $G(E_f)$ and the electron effective mass, $\boldsymbol{m}^*$, as [9], where a is the lattice constant. Since we do not have any detailed knowledge of the effective masses, we can only express the conductivity ratio for the materials, i.e.,

$$\sigma \propto \frac{1}{\boldsymbol{m}^{*2}} (G(E_f))^2$$

where m^*, the density-of-states effective mass, is related inversely to the width of the density-of-states functions, ΔE_f near E_f,

$$\frac{1}{m^*} \propto \Delta E_f.$$

This relation recognises the differential narrowness of the bands in which the Fermi surface lies.

Using these equations, we obtain the relative conductivities for VP, CrP and MnP as:

VP : CrP : MnP : 1.5 : 1.0 : 2.2.

The conductivity for MnP will be further enhanced by the lowering in the number of scattering sites resulting from the magnetic nature of the material. Ripley [10] has measured the specific electrical resistivities of these materials at 20°C and, converting to specific conductivities, the following trend is noted,

VP : CrP : MnP : 2.5 : 1.0 : 10,

which is in line with the predictions above.

The joint-density-of-states functions, J'DOS(E), were also calculated for VP, CrP, and MnP. High intensities in the lower-energy region are found and result from the position of the Fermi level in the d-bands of these compounds. The overall nature of the JDOS(E) functions is similar to the density-of-states functions $G(E)$ and is predicted to match the total absorption or total emission spectra on a qualitative basis.

3.4. Bonding and Charge Separation in VP, CrP, *and* MnP

The well-known results of crystal-field theory with respect to d-orbital splitting in an octahedral field have been applied to energy-band theory through semi-intuitive arguments [3]. It has been assumed that the d-bands in transition -metal compounds can always be split into non-overlapping "e_g" and "t_{2g}" sub-bands, provided that the d-bands are sufficiently narrow and that the crystal field is sufficiently strong. There is thus a tendency to associate the crystal-field splitting in cubic systems with the energy separation between band states at the centre of the Brillouin Zone, namely, those with Γ_{12} and Γ'_{25} symmetry, respectively. Goodenough's theory for transition-metal monophosphides was based on similar arguments and assumes that the $3d$-bands (which lie between the valence band arising from the $3s$ and $3p$ orbitals of phosphorus and an empty conduction band arising from the $4s$ and $4p$ orbitals of the metal) are split into two non-overlapping bands roughly of Γ_{12} and Γ'_{25} character. However, the results of our calculation contrast distinctly these assumptions; firstly (as shown in Fig. 13), we do not find the states arising from the phosphorus $3s$ and $3p$ orbitals lying completely in the valence band. On the contrary, these bands can be spread over the entire energy range, starting from the lowest-lying valence band passing through the Fermi level into the conduction band. A similar trend is found for

the bands arising from the 4*s* and 4*p* orbitals of the metal which are also found in the valence band. It is also interesting that, when the non-metal stems from the 2nd Periodic Group and has 2*s* and 2*p* orbitals, as in the transition-metal oxides, then there does arise a band gap between the bands arising from the oxygen 2*s* and 2*p* orbitals and the metal 3*d* orbitals [11]. This separation of states is typical for systems which are highly polar and the low-lying non-metal states act as a sink for electrons. Hence, in these phosphides the disappearance of the gap between the ligand and the metal bands emphasises the covalent nature of these materials. Secondly, complete splitting of the 3*d*-bands (now overlapped by the bands of *s* and *p* character) into two non-overlapping sub-bands of roughly "t_{2g}" and "e_g" character is not produced. Rather, they cluster

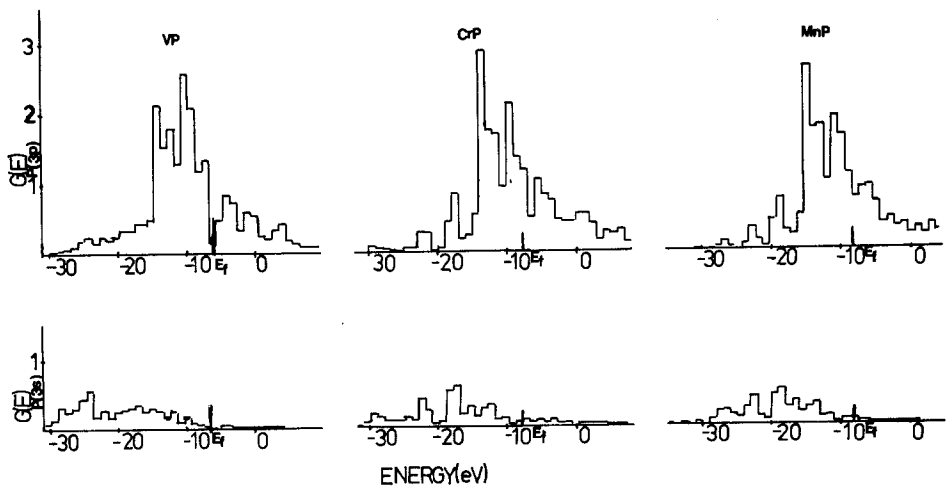

Fig. 13. Partial densities of phosphorus states for VP, CrP, MnP

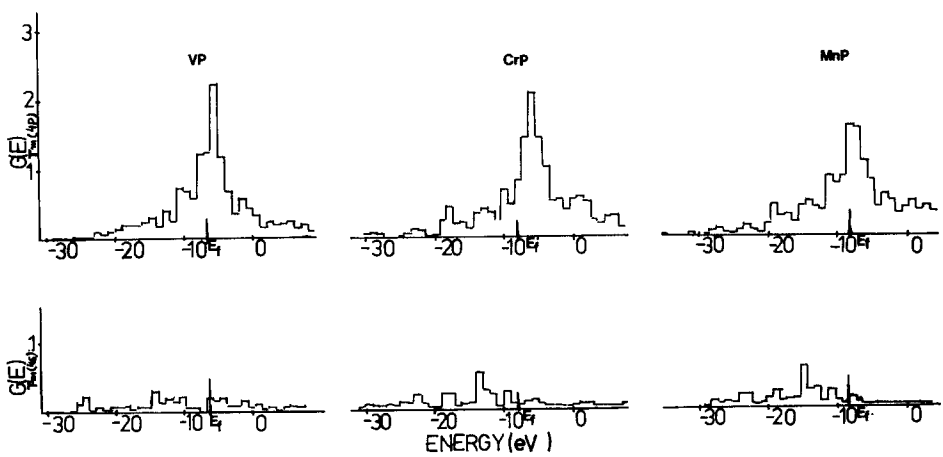

Fig. 14. Partial densities of metal 4*s* and 4*p* states

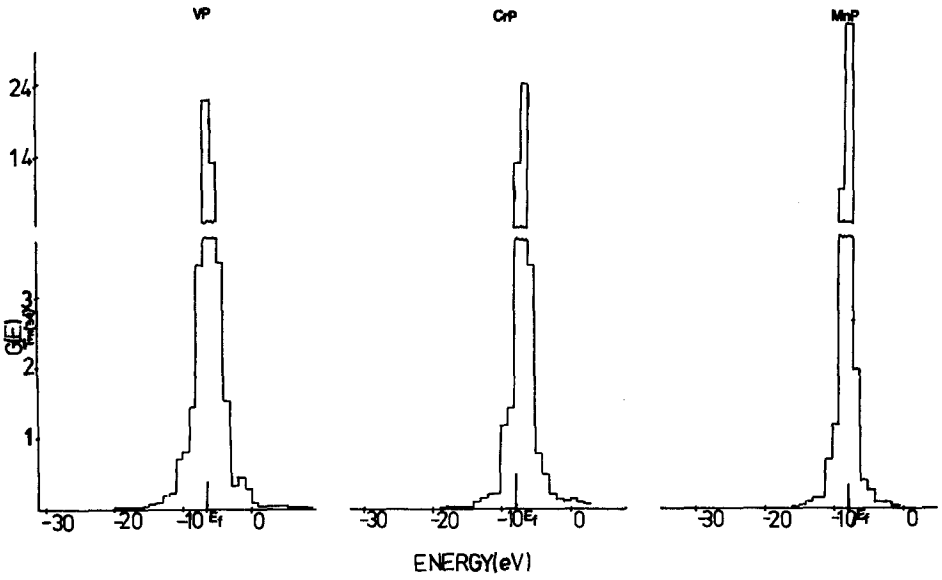

Fig. 15. Partial densities of metal $3d$ states

together over narrow energy ranges for all three phosphides. This is in line with the band-structure results of transition-metal oxides obtained by Mattheiss [11], where he finds the overall d-band width varying from about 6 eV to 4 eV as one moves along the series from VO to NiO.

The computed atomic charges in these compounds are shown in Table 5. Although these values can only be approximate, it is clear that the polarity is far from a limit of $M^{3+}P^{3-}$ (indeed, if the calculation were made self-consistent, these charges would decrease and the bond become even less polar). The calculated negative charge population on the metal atom is a consequence of the diffuse nature of the (mainly $4p$) orbitals of the metal atoms. In reality, the electron density in such diffuse orbitals will spread significantly to the region of the phosphorus atom, thereby effectively reducing the charge separation. Of some interest is the increase in $3d$ population shown by the metal atoms. Here the $3d$ population exceeds that in the free atoms and is in line with the trend found in the metallic crystals of the transition-metal elements [12].

Table 5. Atomic orbital populations and formal charges in MP

	Metal			Phosphorus		Charges	
	$3d$	$4s$	$4p$	$3s$	$3p$	M	P
VP	3.70	0.43	1.27	1.09	3.50	−0.40	+0.40
CrP	5.45	0.60	1.02	0.97	2.96	−1.07	+1.07
MnP	6.14	0.66	1.28	0.97	2.95	−1.06	+1.06

Acknowledgement. One of us (A.K.M.) thanks the University of Strathclyde for a Bursary.

References

1. Perkins, P. G., Marwaha, A. K.,Stewart, J. J. P.: Theoret. Chim. Acta (Bprp.) this volume
2. Stein, B. F., Walinsley, R. H.: Phys. Rev. **148**, 933 (1966)
3. Goodenough, J. B.: Phys. Rev. **117**, 1442 (1960)
4. Rundqvist, S.: Acta Chem. Scand. **16**, 287 (1962)
5. Rundqvist, S.: Arkiv Kemi **20**, 67 (1962)
6. Rundqvist, S.: Acta Chem. Scand. **19**, 1006 (1965)
7. Slater, J. C.: Symmetry and energy bands in crystals. New York: Dover Publication 1972
8. Ziman, J. M.: Electrons and phonons. Oxford: Oxford University Press 1960
9. Molt, N. F., Davis, E. A.: Electronic processes in non-crystalline materials. Oxford: Oxford University Press 1971
10. Ripley, R. L.: J. Less Common Metals **4**, 496 (1962)
11. Mattheis, L. F.: Phys. Rev. **B5**, 290, 306 (1972)
12. Slater, J. C.: Phys. Rev. **49**, 537 (1936)
13. Burns, G.: J. Chem. Phys. **41**, 1521 (1969)

Received September 25, 1980/October 23, 1980/ March 6, 1981